Journal of Materials Chemistry C

Coupling of Charge Carriers with Magnetic Entropy for Power Factor Enhancement in Mn Doped $Sn_{1.03}Te$ for Thermoelectric Applications

Journal:	*Journal of Materials Chemistry C*
Manuscript ID	TC-ART-02-2018-000788.R1
Article Type:	Paper
Date Submitted by the Author:	30-Apr-2018
Complete List of Authors:	Acharya, Somnath; Indian Institute of Technology Mandi, School of Basic Sciences Sharmistha, Anwar; Institute of Minerals and Materials Technology CSIR, Advanced Material Technology Mori, Takao; National Institute for Materials Science, Soni, Ajay; Indian Institute of Technology Mandi, School of Basic Sciences

Coupling of Charge Carriers with Magnetic Entropy for Power Factor Enhancement in Mn Doped $Sn_{1.03}Te$ for Thermoelectric Applications

Somnath Acharya[1], Sharmistha Anwar[2], Takao Mori[3] and Ajay Soni[1]*

[1] *School of Basic Sciences, Indian Institute of Technology Mandi, Mandi, Himachal Pradesh 175005, India*

[2] *Advanced Materials Technology Department, CSIR- IMMT, Bhubaneswar, Odisha 751013, India*

[3] *International Center for Materials Nanoarchitectonics (WPI-MANA), National Institute for Materials Science (NIMS), Namiki 1-1, Tsukuba, 305-0044, Japan.*

* To whom the correspondence should be addressed. Email address: *ajay@iitmandi.ac.in*

Despite being a prospective thermoelectric (TE) material, SnTe has limited applicability due to very high 'hole' concentration arising from 'Sn' vacancies. Engineering of multiple valence band with addition of extra 'Sn' and isovalent doping is a well-established strategy for enhanced TE properties. Here, we report a new approach utilizing magnetism to try to enhance the TE properties. Magnetic and TE properties of Mn doped self-compensated $Sn_{1.03}Te$ were studied in context of its dilute magnetic nature. A systematic (i) increment of magnetic moments and weak ferromagnetism leading to coupling of charge carriers, (ii) increase in effective thermal mass of charge carriers and (iii) overall enhancements in power factor has been observed and analyzed based on the magnetization, heat capacity and high temperature transport measurements. At low temperatures weak ferromagnetism is generated with Mn doping in otherwise diamagnetic $Sn_{1.03}Te$, thus giving system magnetic entropy and structural disorders which leads to a modified TE transport. Enhancement of power factor for $Sn_{0.93}Mn_{0.1}Te$ from $Sn_{1.03}Te$ has been explained based on magnetic moments, anomalous Hall Effect, high effective thermal mass and magnetic entropy.

Introduction

Being emission-free, silent, vibration-less and without scaling effect, thermoelectric (TE) generators are expected to play a vital role in energy harvesting techniques via direct conversion of waste heat into electrical energy.[1] Conversion efficiency of any TE material can be estimated by using dimensionless figure of merit, $ZT = \alpha^2\sigma T/(\kappa_e + \kappa_l)$, where α is thermoelectric power, σ is electrical conductivity, κ_e is electronic thermal conductivity, κ_l is lattice thermal conductivity and T is an average absolute temperature, respectively. Enhancement of ZT has been limited in a certain range of carrier concentration n, due to mutual correlation of three TE parameters. To attain high ZT, decoupling of electrical and thermal transport is one of the most crucial aspects for enhancing power factor, $\alpha^2\sigma$ and lowering thermal conductivity, κ. [2-5] Poor κ has been achieved by solid solution alloying,[6] nanostructuring,[7, 8] rattling atoms,[9] softening of phonons,[10, 11] nano-micropores,[12] and introducing defects[13] while enhancing $\alpha^2\sigma$ is more challenging as α and σ are strongly dependent on electronic band structure around density of states near Fermi energy. Valence bands convergence[14, 15] and introducing resonant states[16, 17] in valence bands have remarkably improved $\alpha^2\sigma$ by enhancing α while maintaining an optimized σ.

Tin telluride (SnTe) is a group IV-VI narrow-gap semiconductor with a high n originating from inherent Sn vacancies.[18-23] The high n can be controlled by self-substitution of Sn and/or doping with guest elements.[11, 21, 24, 25] Sn-Mn-Te belongs to a family of dilute magnetic semiconductor such as Pb-Mn-Te, Pb-Mn-Se, Pb-Mn-S and Pb-Sn-Mn-Te where Mn^{2+} ions carry localized spin magnetic moments (S = 5/2).[26, 27, 28] Mn being divalent not only provides an optimized density of state for light and heavy hole valence bands through charge carrier modification,[21, 29, 30] but also gives rise to soft phonon modes[11] by structural anharmonicity to modify the TE properties. The effect of magnetic element doping and utilization of magnetic interactions [28 31-33] has been shown

to be a unique strategy to enhance the carrier effective mass and enhance TE performance of materials. In addition to this, inclusion of superparamagnetic nanoparticles in matrix[34] and magnon drag effects at low temperatures in magnetically ordered systems[35-37] have also been reported for improvements in TE properties.

In this work, we report charge carrier coupled magnetic moments with high $\alpha^2\sigma$ in Mn doped self-compensated $Sn_{1.03}Te$. The high $\alpha^2\sigma$ attributes to contribution from high n and enhanced effective mass by coupling of charge carriers and magnetic moments, which is supported by temperature and field dependent magnetic, anomalous Hall Effect and heat capacity measurements.

Experimental Details

Polycrystalline $Sn_{1.03-x}Mn_xTe$ (x = 0, 0.05, 0.07 and 0.1) samples were synthesized by solid-state melting method using high purity Sn powder (99%), Te shot (99.99%) and Mn chips (99.99%) in the stoichiometric ratio and the details on preparation and characterizations can be found in earlier work.[11] To a brief note, vacuum sealed (~ 10^{-5} mbar) samples were heated to 1073 K and soaked for 6 h followed by quenching in water. The obtained ingots grounded to powder and cold pelletized followed by vacuum annealing at 773 K for 72 h. Temperature and magnetic field dependent magnetization measurements were performed using a superconducting quantum interference magnetometer, (SQUID-MPMS-3, Quantum Design). Physical properties measurements system (PPMS-Dyna cool, Quantum Design) was used for both heat capacity and Hall Effect measurements. High temperature α and σ measurements were performed on a bar shaped samples (dimension ~ 3 mm x 2 mm x 10 mm), using a ULVAC ZEM-3.

Results and Discussion

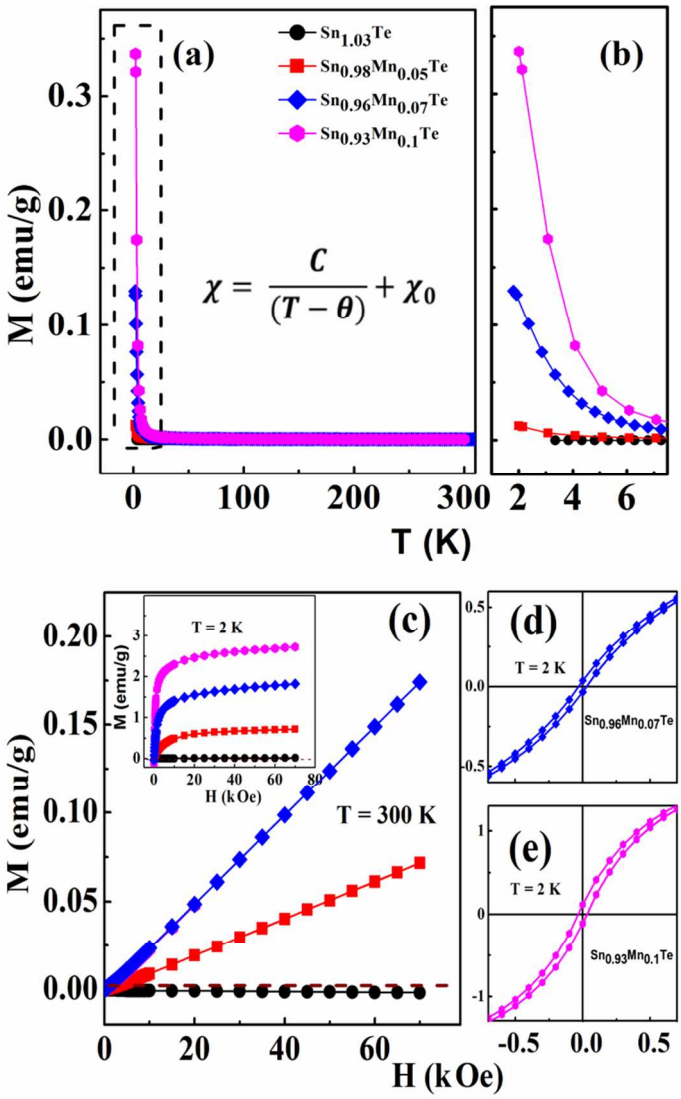

Fig. 1. (a) *M (T)* with Mn content showing paramagnetic response in temperature range of 2-350 K, (b) expanded view of *M (T)* in a narrow range of 2-8 K, (c) *M (H)* plot with Mn content at 300 K and 2 K (inset); (d) and (e) are low field *M (H)* at 2 K for $Sn_{0.96}Mn_{0.07}Te$ and $Sn_{0.93}Mn_{0.1}Te$, respectively, showing a very weak ferromagnetism. All figures share same color notation for sample identification.

To understand the magnetism originating from Mn doping, temperature dependent magnetization, *M (T)*, at 100 Oe field is shown in Fig. 1(a). *M (T)* of pure $Sn_{1.03}Te$ shows a diamagnetic behavior with temperature independent and negligible negative values, while Mn doped samples show a systematic paramagnetic behavior throughout the temperature range of 2-350 K. Noticeably, *M* values increases with Mn content below 8 K, (Fig. 1(b)). Further, negative field dependence of *M (H)*, of $Sn_{1.03}Te$ in Fig 1(c), both at 2 and 300 K, clarifies the weak diamagnetic response. For Mn doped samples, linear *M (H)* suggest a strong paramagnetic response at 300 K, whereas saturation in *M (H)* (Inset, Fig. 1(c)) and existence a feeble coercivity ($H_c \sim$ 60-80 Oe), (Fig. 1(d) and (e)) demonstrate a very weak ferromagnetism at 2 K, for $Sn_{0.96}Mn_{0.07}Te$ and $Sn_{0.93}Mn_{0.1}Te$, respectively. Thus, Mn is providing a systematic magnetic ordering, which is expected to develop indirect exchange interaction with charge carriers and modify charge transport properties. For a ferromagnet in paramagnetic region, magnetic susceptibility $\chi\ (= {}^{M}/_{H})$, is expressed by a Curie-Weiss fuctions, $\chi = \frac{C}{(T-\theta)} + \chi_0$, where C, θ, and χ_0 are the Curie constant, paramagnetic Curie temperature, and a temperature independent diamagnetic term, respectively.[38] Here, the Curie constant is given as $C = N_{Mn}\mu_{eff}^2 /3k_B$, where N_{Mn} is the number of Mn atoms, μ_{eff} *is* the effective magnetic moment, usually given in units of μ_B, the Bohr magneton. The μ_{eff} determined from the Curie-Weiss fits and the approximate saturation magnetization μ_s (estimated from the magnetization at 2 K measured at the maximum field 70 k Oe) are given in Table 1, as a function of Mn doping. Values of μ_{eff} are substantial,[28] indicating that the magnetization is derived from the doped Mn atoms and not from any minor impurity phase. The small values of saturation magnetization indicate the itinerant nature of magnetism. Thus, all magnetic data provide evidence

for weak ferromagnetism in doped $Sn_{1.03-x}Mn_xTe$ samples, which can affect charge transport in these samples.

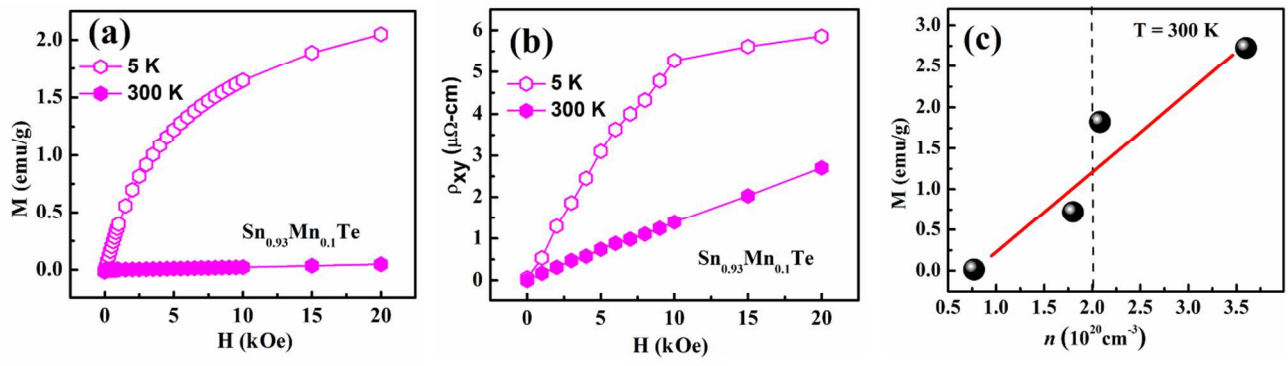

Fig. 2. (a) *M (H)* and (b) Hall resistivity, ρ_{xy} *(H)* of $Sn_{0.93}Mn_{0.1}Te$ at 5 K (open circle) and 300 K (solid circle). (c) *M* as function of *n* (or Mn content) at 300 K. Solid line is guide to the eyes and vertical dashed line indicates threshold *n*.

In metals and degenerate semiconductors, the Lorentz force drives charge carriers to exhibit a linear transverse Hall voltages with applied magetic field. Whereas, in the case of magnetic materials or in the presence of magnetic impurites, Hall voltage has non-linear dependence with external field (known as Anomalous Hall Effect-AHE). The non-linearity is because of internal fields.[39, 40] Thus, AHE is one of the important tool to understand coupling between charge carriers and magnetic moments. *M (H)* and Hall resistivity, ρ_{xy} *(H)* at 5 and 300 K of $Sn_{0.93}Mn_{0.01}Te$, are shown in Fig. 2 (a) and (b), respectivly. A very strong non-linear ρ_{xy} *(H)* is observed at 5 K, whereas a linear ρ_{xy} *(H)* at 300 K. Non-linear field dependence appears due to internal field arising from magnetization in addition to applied field, thus described with two terms, $\rho_{xy} = R_0H + 4\pi MR_s$, where R_0 and R_s are ordinary and anomalous Hall coefficients, respectively, and *M* is

magnetization.[41] First term represents normal Hall effect due to Lorenz force on charge carriers, while second term refers to the anomalous Hall effect, which is temperature dependent and proportional to magnetization.[39] A large AHE is observed in magnetic semiconducters, especially ferromagnetic materials such as $Ga_{1-x}Mn_xAs$,[42] $Fe_{1-x}Co_xSi$[40] and also observed for the magnetic semiconductor $CuGa_{1-x}Mn_xTe_2$.[31] Notably, the estimated $R_0 = 0.56 \times 10^{-4}$ μΩ-cm G^{-1} and $R_s = 0.39$ μΩ-cm G^{-1} values suggest the strong magnetic coupling between charge carriers and Mn moments.[39] Here, positive values of R_s suggest weak ferromagnetism in samples.[31] AHE is a result of strong assymetric scattering of charge carriers with local moments and this scattering is high for materials with high n. Comparing with earlier reports on Mn-doped SnTe thin films, the threshold n for ferromagnetism is $n_t \approx 2 \times 10^{20}$ cm^{-3}, which is the case with our sample too. As shown in Fig. 2(c), samples with n lower than n_t show low M values whereas samples higher than n_t show magnetic ordering with enhanced M values. The threshold n_t is equal to the concentration of carriers at which the Fermi level enters the band of heavy holes, thus the magnetic moments due to Mn are coupled to n in $Sn_{1.03-x}Mn_xTe$.[43]

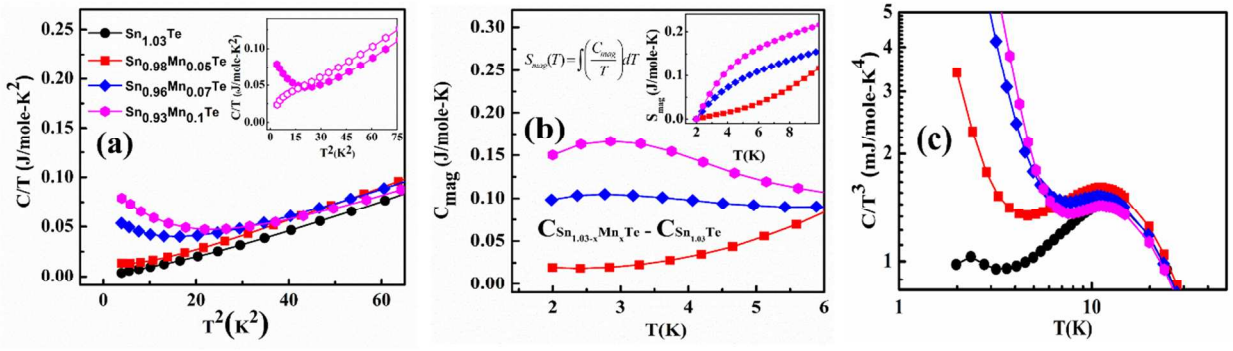

Fig. 3. (a) C/T versus T^2 plot with Mn content, upturn below 6 K is appearing in Mn doped samples; Inset shows that with application of 50 k Oe magnetic field upturn vanishes for $Sn_{0.93}Mn_{0.1}Te$, (b) magnetic contribution C_{mag} from Mn, is estimated by subtracting C ($Sn_{1.03}Te$)

from C ($Sn_{1.03-x}Mn_xTe$); Inset shows estimated magnetic entropy and (c) log-log plot of C/T^3 versus T. All figures share same color notation for sample identification.

Table 1. Parameters derived from magnetic and specific heat data of $Sn_{1.03-x}Mn_xTe$.

Sample Name	Magnetization		Heat capacity		
	μ_{eff} (μ_B/Mn)	$\mu_{s.}$ (μ_B/Mn)	γ ($mJK^{-2}mol^{-1}$)	β ($mJK^{-4}mol^{-1}$)	θ_D (K)
$Sn_{1.03}Te$	-	-	0.2	0.95	160
$Sn_{0.98}Mn_{0.05}Te$	2.9	0.64	4.4	1.18	149
$Sn_{0.96}Mn_{0.07}Te$	4.4	1.1	6.3	1.27	145
$Sn_{0.93}Mn_{0.1}Te$	3.1	1.2	7.0	1.35	142

In earlier reports, appearance of soft-phonon modes in Raman spectra of doped samples were indicated to give rise to anharmonicity in samples, and consequently a low thermal conductivity was reported.[11] To understand the effect of magnetism on thermal transport, we carried out heat capacity measurements at low temperatures. All Mn doped samples exhibit upturns below ~ 8 K in the molar heat capacity C/T vs T^2 curves (Fig. 3 (a)), which substantially disappear under 50 k Oe magnetic field (Inset, Fig. 3). This indicates that the associated contribution originates from the weak ferromagnetism in samples. Furthermore, excluding the heat capacity below 6 K, electronic and lattice contributions have been estimated by fitting data with $C/T = \gamma + \beta T^2$, where γ is Sommerfield constant and β is lattice part to heat capacity.[44] The Debye temperature can be estimated using $\theta_D = \left(\frac{12\pi^4 NR}{5\beta}\right)^{1/3}$, where N is the number of atoms per formula unit (here $N = 2$) and $R \approx 8.314$ J mol^{-1} K^{-1} is the ideal gas constant.[44] The estimated γ, β and θ_D values from fitting results are listed in Table 1. The estimated θ_D values are in range of 142 to 160 K, which is consistent with reported values of SnTe.[45] Systematic increase of γ with Mn doping can be

understood as due to enhanced effective mass of carriers with magnetic ordering. Magnetic contribution to heat capacity (C_{mag}) is estimated by subtracting C of $Sn_{1.03}Te$ from C of Mn doped samples and finally magnetic entropy $S_{mag}(T) = \int \left(\frac{C_{mag}}{T} \right) dT$, has been calculated (Fig. 3 (b) and inset). A systematic increase in both C_{mag} and S_{mag} confirms the effect of magnetism on thermal transport. In addition to electronic and magnetic contributions to heat capacity, soft phonon modes[11] and structural disorder due to Mn-doping also affect the lattice contributions of heat capacity. Lattice contribution due to disorders can be analyzed by plotting C/T^3 vs T, which is used to understand nature of phonons in disordered metals, metallic glasses[46] and charge ordered states in compounds.[47] A hump like feature, called boson peak,[46] is observed and low temperature data diverges with higher Mn content which is a signature of the existence of low energy contributions to thermal transport.[47] In case of amorphous and crystalline conductors, these low energy vibrations cannot be accounted by usual Debye model.[46] This behavior has agreement with previously reported soft-phonon modes affecting the thermal transport in SnMnTe.[11] Thus, increased magnetic entropy as well as disorder from Mn significantly modifies thermal behavior of samples.

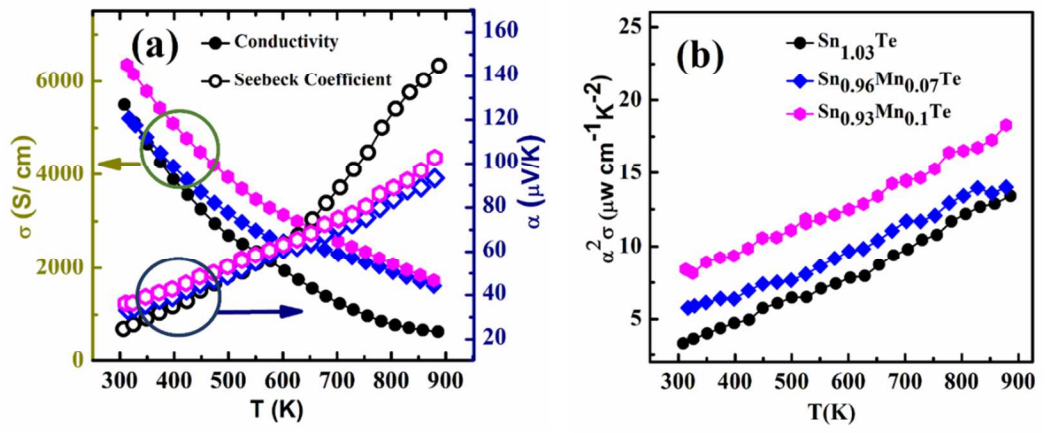

Fig. 4. Temperature dependence of (a) σ (closed symbol), α (open symbol) and (b) $\alpha^2\sigma$ of Mn doped $Sn_{1.03}Te$ samples. Color notations of samples are shown in (b).

To understand further on the overall effect of magnetic interactions on TE properties of $Sn_{1.03-x}Mn_xTe$, temperature dependent TE transport measurements (σ, α and $\alpha^2\sigma$) have been performed in the range of 325 - 873 K (Fig. 4). In all samples, σ decreases with increasing temperature showing a metallic nature, while increase in α is attributed to high carrier effective mass supported by γ values and convergence of double valence bands.[11] In previous reports, different dopants (Cd, Hg, Mg and Mn) are used for engineering the degeneracy of light hole and heavy hole valence bands to achive high α.[21, 25, 48] Therefore, with Mn doping, high α and σ can be explained from enhanced carrier effective mass and large n respectively. Consequently, we have discovered that $\alpha^2\sigma$ of Mn-doped samples is enhanced three times for $Sn_{0.93}Mn_{0.1}Te$ with respect to $Sn_{1.03}Te$, via enhancing the effective carrier mass because of interaction between charge carriers and magnetic moments.

Conclusions

In summary, we have demonstrated the effect of weak ferromagnetism on TE transport properties of Mn doped self-compensated $Sn_{1.03}Te$. Interaction between magnetic moments of Mn and charge carriers in $Sn_{1.03-x}Mn_xTe$ has been indicated by analysis of the weak ferromagnetism and anomalous Hall effect, which results in an enhancement of the power factor $\alpha^2\sigma$ by three times. Here the role of Mn is not only to provide structural disorders but also to give magnetic coupling of charge carriers by assymetric scattering. We emphasize that we have realised an effective strategy for better TE properties with Mn doping in this system, developing anharmonicity in lattice while enhancing effective mass of carriers through magnetic entropy.

Acknowledgements

AS would like to acknowledge Board of Research in Nuclear Sciences, India for young scientist research award (37(3)/14/02/2015/BRNS), DST-SERB (YSS/2014/001038) and Advanced Material Research Centre, Indian Institute of Technology Mandi for research facility. TM thanks Japan Science and Technology Agency (JST) CREST Grant No. JPMJCR15Q6.

References

1. K. Biswas, J. He, I. D. Blum, C.-I. Wu, T. P. Hogan, D. N. Seidman, V. P. Dravid and M. G. Kanatzidis, *Nature*, 2012, **489**, 414-418.
2. G. D. Mahan, *APL Materials*, 2016, **4**, 104806.
3. T. Zhu, Y. Liu, C. Fu, J. P. Heremans, J. G. Snyder and X. Zhao, *Advanced Materials*, 2017, DOI: 10.1002/adma.201605884, 1605884.
4. W. Liu, H. S. Kim, Q. Jie and Z. Ren, *Scripta Materialia*, 2016, **111**, 3-9.
5. T. Mori, *Small*, 2017, **13**, 1702013.
6. G. Tan, W. G. Zeier, F. Shi, P. Wang, G. J. Snyder, V. P. Dravid and M. G. Kanatzidis, *Chemistry of Materials*, 2015, **27**, 7801-7811.
7. A. J. Minnich, M. S. Dresselhaus, Z. F. Ren and G. Chen, *Energy & Environmental Science*, 2009, **2**, 466-479.
8. A. Soni, Z. Yanyuan, Y. Ligen, M. K. K. Aik, M. S. Dresselhaus and Q. Xiong, *Nano Letters*, 2012, **12**, 1203-1209.
9. M. Beekman, D. T. Morelli and G. S. Nolas, *Nat Mater*, 2015, **14**, 1182-1185.
10. S. Lee, K. Esfarjani, T. Luo, J. Zhou, Z. Tian and G. Chen, *Nature Communications*, 2014, **5**, 3525.

11. S. Acharya, J. Pandey and A. Soni, *Applied Physics Letters*, 2016, **109**, 133904.
12. A. U. Khan, K. Kobayashi, D.-M. Tang, Y. Yamauchi, K. Hasegawa, M. Mitome, Y. Xue, B. Jiang, K. Tsuchiya, D. Golberg, Y. Bando and T. Mori, *Nano Energy*, 2017, **31**, 152-159.
13. Z. Li, C. Xiao, H. Zhu and Y. Xie, *Journal of the American Chemical Society*, 2016, **138**, 14810-14819.
14. Y. Pei, X. Shi, A. LaLonde, H. Wang, L. Chen and G. J. Snyder, *Nature*, 2011, **473**, 66-69.
15. Y. Pei, H. Wang and G. J. Snyder, *Advanced Materials*, 2012, **24**, 6125-6135.
16. J. P. Heremans, V. Jovovic, E. S. Toberer, A. Saramat, K. Kurosaki, A. Charoenphakdee, S. Yamanaka and G. J. Snyder, *Science*, 2008, **321**, 554-557.
17. L. Wang, X. Tan, G. Liu, J. Xu, H. Shao, B. Yu, H. Jiang, S. Yue and J. Jiang, *ACS Energy Letters*, 2017, **2**, 1203-1207.
18. R. F. Brebrick, *Journal of Electronic Materials*, 1977, **6**, 659-692.
19. S. Acharya and A. Soni, *AIP Conference Proceedings*, 2017, **1832**, 110028.
20. G. Tan, L.-D. Zhao, F. Shi, J. W. Doak, S.-H. Lo, H. Sun, C. Wolverton, V. P. Dravid, C. Uher and M. G. Kanatzidis, *J. Am. Chem. Soc.*, 2014, **136**, 7006-7017.
21. A. Banik, U. S. Shenoy, S. Anand, U. V. Waghmare and K. Biswas, *Chemistry of Materials*, 2015, **27**, 581-587.
22. A. Banik, B. Vishal, S. Perumal, R. Datta and K. Biswas, *Energy & Environmental Science*, 2016, **9**, 2011-2019.
23. A. Banik and K. Biswas, *Journal of Materials Chemistry A*, 2014, **2**, 9620-9625.
24. M. Zhou, Z. M. Gibbs, H. Wang, Y. Han, C. Xin, L. Li and G. J. Snyder, *Physical Chemistry Chemical Physics*, 2014, **16**, 20741-20748.

25. G. Tan, L.-D. Zhao, F. Shi, J. W. Doak, S.-H. Lo, H. Sun, C. Wolverton, V. P. Dravid, C. Uher and M. G. Kanatzidis, *Journal of the American Chemical Society*, 2014, **136**, 7006-7017.

26. T. Story, G. Karczewski, L. Świerkowski and R. R. Gałązka, *Physical Review B*, 1990, **42**, 10477-10487.

27. P. Łazarczyk, T. Story, M. Arciszewska and R. R. GaŁzka, *Journal of Magnetism and Magnetic Materials*, 1997, **169**, 151-158.

28. H. Chi, G. Tan, M. G. Kanatzidis, Q. Li and C. Uher, *Applied Physics Letters*, 2016, **108**, 182101.

29. J. He, X. Tan, J. Xu, G.-Q. Liu, H. Shao, Y. Fu, X. Wang, Z. Liu, J. Xu, H. Jiang and J. Jiang, *Journal of Materials Chemistry A*, 2015, **3**, 19974-19979.

30. W. Li, Z. Chen, S. Lin, Y. Chang, B. Ge, Y. Chen and Y. Pei, *Journal of Materiomics*, 2015, **1**, 307-315.

31. F. Ahmed, N. Tsujii and T. Mori, *Journal of Materials Chemistry A*, 2017, **5**, 7545-7554.

32. N. Tsujii and T. Mori, *Applied Physics Express*, 2013, **6**, 043001.

33. A. U. Khan, R. A. R. A. Orabi, A. Pakdel, J.-B. Vaney, B. Fontaine, R. Gautier, J.-F. Halet, S. Mitani and T. Mori, *Chemistry of Materials*, 2017, **29**, 2988-2996.

34. W. Zhao, Z. Liu, Z. Sun, Q. Zhang, P. Wei, X. Mu, H. Zhou, C. Li, S. Ma, D. He, P. Ji, W. Zhu, X. Nie, X. Su, X. Tang, B. Shen, X. Dong, J. Yang, Y. Liu and J. Shi, *Nature*, 2017, **549**, 247.

35. K. Vandaele, S. J. Watzman, B. Flebus, A. Prakash, Y. Zheng, S. R. Boona and J. P. Heremans, *Materials Today Physics*, 2017, **1**, 39-49.

36. S. R. Boona, S. J. Watzman and J. P. Heremans, *APL Materials*, 2016, **4**, 104502.

37. R. Ang, A. U. Khan, N. Tsujii, K. Takai, R. Nakamura and T. Mori, *Angewandte Chemie International Edition*, 2015, **54**, 12909-12913.

38. B. D. Cullity and D. D. Graham, *Introduction to Magnetic Materials* Wiley-IEEE Press, 2nd edn., 2008.

39. P. Łazarczyk, T. Story, A. Jędrzejczak, R. R. Gałązka, W. Mac, M. Herbich and A. Stachow-Wójcik, *Journal of Magnetism and Magnetic Materials*, 1997, **176**, 233-240.

40. N. Manyala, Y. Sidis, J. F. DiTusa, G. Aeppli, D. P. Young and Z. Fisk, *Nat Mater*, 2004, **3**, 255-262.

41. C. M. Hurd, *The Hall Effect in Metals and Alloys* Plenum Press, New York, 1972.

42. F. Matsukura, H. Ohno, A. Shen and Y. Sugawara, *Physical Review B*, 1998, **57**, R2037-R2040.

43. T. Story, R. R. Gałązka, R. B. Frankel and P. A. Wolff, *Physical Review Letters*, 1986, **56**, 777-779.

44. C. Kittel, *Introduction to Solid State Physics*, Wiley, 2004.

45. D. H. Damon, *Journal of Applied Physics*, 1966, **37**, 3181- 3190.

46. D. J. Safarik, R. B. Schwarz and M. F. Hundley, *Physical Review Letters*, 2006, **96**, 195902.

47. R. Yoshimoto, Y. Takane, K. Hino, S. Yamashita and Y. Nakazawa, *Physica B: Condensed Matter*, 2014, **449**, 19-24.

48. G. Tan, F. Shi, J. W. Doak, H. Sun, L.-D. Zhao, P. Wang, C. Uher, C. Wolverton, V. P. Dravid and M. G. Kanatzidis, *Energy & Environmental Science*, 2015, **8**, 267-277.

Coupling of Charge Carriers with Magnetic Entropy for Power Factor Enhancement in Mn Doped $Sn_{1.03}Te$ for Thermoelectric Applications

Somnath Acharya[1], Sharmistha Anwar[2], Takao Mori[3] and Ajay Soni[1]*

[1] *School of Basic Sciences, Indian Institute of Technology Mandi, Mandi, Himachal Pradesh 175005, India*

[2] *Advanced Materials Technology Department, CSIR- IMMT, Bhubaneswar, Odisha 751013, India*

[3] *International Center for Materials Nanoarchitectonics (MANA), National Institute for Materials Science (NIMS), Namiki 1-1, Tsukuba, 305-0044, Japan.*

* To whom the correspondence should be addressed. Email address: *ajay@iitmandi.ac.in*

Table of Content (ToC)